

AD-A104 033

ARMY ARMAMENT RESEARCH AND DEVELOPMENT COMMAND ABERD--ETC F/G 20/14  
A FLOW MODEL FOR THE EFFECT OF A SLANTED BASE ON DRAG. (U)

JUL 81 R SEDNEY

UNCLASSIFIED

ARBRRL-TR-02341

NL

1 or 1  
ADA  
F/G 20/14

END  
DATE  
FILED  
10-81  
DTIC

AD A104033

12

LEVEL II <sup>BS</sup>

AD

TECHNICAL REPORT ARBRL-TR-02341 ✓

A FLOW MODEL FOR THE EFFECT OF A  
SLANTED BASE ON DRAG

Raymond Sedney

July 1981

DTIC  
ELECTED  
SEP 10 1981  
S D  
B



US ARMY ARMAMENT RESEARCH AND DEVELOPMENT COMMAND  
BALLISTIC RESEARCH LABORATORY  
ABERDEEN PROVING GROUND, MARYLAND

Approved for public release; distribution unlimited.

DTIC FILE COPY

81 9 09 101

Destroy this report when it is no longer needed.  
Do not return it to the originator.

Secondary distribution of this report by originating  
or sponsoring activity is prohibited.

Additional copies of this report may be obtained  
from the National Technical Information Service,  
U.S. Department of Commerce, Springfield, Virginia  
22161.

The findings in this report are not to be construed as  
an official Department of the Army position, unless  
so designated by other authorized documents.

*The use of trade names or manufacturers' names in this report  
does not constitute endorsement of any commercial product.*

## UNCLASSIFIED

SECURITY CLASSIFICATION OF THIS PAGE (When Data Entered)

REPORT DOCUMENTATION PAGE		READ INSTRUCTIONS BEFORE COMPLETING FORM
1. REPORT NUMBER TECHNICAL REPORT, ARBRL-TR-02341	2. GOVT ACCESSION NO. AD-A104 033	3. RECIPIENT'S CATALOG NUMBER
4. TITLE (and Subtitle) A FLOW MODEL FOR THE EFFECT OF A SLANTED BASE ON DRAG .	5. TYPE OF REPORT & PERIOD COVERED Final	
7. AUTHOR(s) Raymond/Sedney	8. CONTRACT OR GRANT NUMBER(s)	
9. PERFORMING ORGANIZATION NAME AND ADDRESS U.S. Army Ballistic Research Laboratory (ATTN: DRDAR-BLL) Aberdeen Proving Ground, Maryland 21005	10. PROGRAM ELEMENT, PROJECT, TASK AREA & WORK UNIT NUMBERS RDT&E 1L161102AH43	
11. CONTROLLING OFFICE NAME AND ADDRESS US Army Armament Research & Development Command US Army Ballistic Research Laboratory (DRDAR-BL) Aberdeen Proving Ground, MD 21005	12. REPORT DATE JULY 1981	
14. MONITORING AGENCY NAME & ADDRESS (if different from Controlling Office)	13. NUMBER OF PAGES 30	
16. DISTRIBUTION STATEMENT (of this Report)  Approved for public release; distribution unlimited.		
17. DISTRIBUTION STATEMENT (of the abstract entered in Block 20, if different from Report)		
18. SUPPLEMENTARY NOTES		
19. KEY WORDS (Continue on reverse side if necessary and identify by block number) Drag Base Drag Vehicle Drag Vortices Vortex Breakdown		
20. ABSTRACT (Continue on reverse side if necessary and identify by block number) Experiments by Morel have shown that slanting the base of a bluff body causes large variations in the drag, as the slant angle changes. For a particular, critical slant angle the drag changes discontinuously. This phenomenon was correlated with a drastic change in the type of base flow. A mechanism to explain this change, and therefore, the discontinuity in drag, is proposed. The basis of the mechanism is breakdown of the side edge vortices. An estimate of the swirl angle in these vortices is obtained using a swept-back mixing zone solution. This swirl angle and the other elements of the		

31111

L12

UNCLASSIFIED

SECURITY CLASSIFICATION OF THIS PAGE(When Data Entered)

2<sup>n</sup>. ABSTRACT (Continued)

theory provide an estimate for the critical slant angle that is entirely consistent with the observed value.

2

UNCLASSIFIED

SECURITY CLASSIFICATION OF THIS PAGE(When Data Entered)

## TABLE OF CONTENTS

	<u>Page</u>
LIST OF ILLUSTRATIONS.....	5
I. INTRODUCTION.....	7
II. THE EXPERIMENTAL EVIDENCE.....	8
III. THE SIDE EDGE FLOW.....	9
IV. THE VORTEX BREAKDOWN HYPOTHESIS.....	11
V. DISCUSSION.....	14
REFERENCES.....	16
LIST OF SYMBOLS.....	23
DISTRIBUTION LIST.....	25

Accession No.	1
NTIS G-111	
REF ID:	
UNIVERSITY	
JULY 1962	
PERIODICAL	
BY THE	
ANNUAL	
Dist	
A	

## LIST OF ILLUSTRATIONS

<u>Figure</u>		<u>Page</u>
1      Models Tested by Morel (Reference 2). Dimensions in mm.....		17
2      Drag Coefficient of the Vehicle-Like Model in the Free Stream Location, From Reference 2.....		17
3      The Two Types of Base Flows for a Body with a Slanted Base...		18
4      Rear View of a Slanted Base Showing Part of the Surface Flow Pattern. The Flow Along the Side (Out of the Plane of the Paper) Separates at the Side Edge and Reattaches at the Dashed Line. Sketched from a Photograph in Reference 3.....		18
5      A Wedge, Semi-Infinite in the $y$ -Direction, as an Idealized Configuration for Side Edge Flow. The Free Stream Velocity, $U$ , is Parallel to the Top and the Side. The Slanted Base is $z = 0$ , $x > 0$ , $y > 0$ .....		19
6      Flow Over an Infinite, Yawed Side Edge at $y = 0$ , $z = 0$ .....		20
7      Vortex Breakdown in a Duct Flow, Made Visible with Dye Introduced into the Flow, from Reference 6. B is the Breakdown Point.....		21

## I. INTRODUCTION

In the search to reduce drag of road vehicles, it has become clear that a more basic understanding of the complex flows about such bodies is required. Many investigations of drag and flow phenomena exist; see Reference 1 for surveys of recent work.

A particularly interesting phenomenon is the effect that slanting the base has on the drag of a bluff body. Following up on work by Janssen and Hucho, partially reported in Reference 1, Morel did a comprehensive study of that effect, see References 1 and 2. Janssen and Hucho observed an overshoot in drag and a change in separation pattern in tests on a model of a hatch-back car, when the angle of the slanted portion of the roof was varied over a small range. In order to examine this effect more closely and gain some understanding of it, Morel<sup>1,2</sup> made extensive tests on two models (see Figure 1): (i) an ogive cylinder with a slanted base, mounted in the center of a wind tunnel to minimize wall effects; and (ii) a vehicle-like model simulating a hatch-back car, mounted in the center of the tunnel and close to the tunnel wall. Because the wind tunnel models are simpler to discuss and there are more experimental details, the results of Morel will be used in this paper.

The most striking result from the tests of Morel was the extremely rapid change in drag coefficient,  $C_D$ , as the slant angle,  $\beta$ , is varied. In fact the data show, essentially, a discontinuity in  $C_D$  for a certain  $\beta = \beta_c$ . Also, for  $\beta < \beta_c$ , the variation of  $C_D$  with  $\beta$  is much greater than for  $\beta > \beta_c$ . The results of Janssen and Hucho are qualitatively the same, but the variation of  $C_D$  with  $\beta$  is smooth, i.e., no discontinuity. (The term discontinuity is used here for convenience and its descriptive accuracy, even though a mathematical discontinuity does not exist.)

Visualizing the flow with smoke, Morel showed that there are two distinct types of base flow. For  $\beta > \beta_c$  a closed base flow, typical of blunt-based axisymmetric bodies, was found. For  $\beta < \beta_c$  streamwise vortices were formed at the side edges with a resultant 3-D separation pattern. It was concluded that switching from one separation pattern to the other caused the discontinuity in  $C_D$ .

---

1. Sovran, G., Morel, T., and Mason, Jr., W.T., Aerodynamic Drag Mechanisms of Bluff Bodies and Road Vehicles, Symposium held at the General Motors Research Laboratories, Plenum Press, New York, 1978.
2. Morel, T., "Aerodynamic Drag on Bluff Body Shapes Characteristic of Hatch-Back Cars", Research Publication GMR-2581, General Motors Research Laboratories, November 1977. See also S.A.E. Technical Paper 780267, 1978.

Additional evidence for the existence of the streamwise vortices springing from the side edges is given by Carr<sup>3</sup>. He used the surface indicator (oil flow) method to visualize the flow and found clear and distinct edge vortices for  $\beta = 25^\circ$  but not for  $\beta = 35^\circ$ . Carr also discusses the downwash produced by, and the effect on the rear lift force of, the side edge vortices.

The primary purpose of this paper is to propose a flow mechanism to explain the change in separation pattern and the discontinuity in  $C_D$ . The mechanism involves breakdown of the side-edge vortices. Vortex breakdown has been relatively well studied and is partially understood; the work on this subject through 1972 has been reviewed by Hall<sup>4</sup>, and later work by Leibovich<sup>5</sup>. To make use of the empirical knowledge on vortex breakdown, a model for the flow over a side edge is required. For an idealized side edge configuration, a flow model is constructed which allows a simple estimate of the swirl in the vortex. Empirical evidence shows that breakdown occurs for a value of swirl corresponding to  $\beta = \beta_c$ , approximately. The consistency of this theoretical result and the experimental data is sufficient to warrant further examination of this mechanism and to test it in additional experiments.

## II. THE EXPERIMENTAL EVIDENCE

For the two models tested by Morel, see Figure 1, the  $\beta_c$  were different. It is simpler to discuss the vehicle-like model because it has a straight side edge. Some discussion of the ogive-cylinder model is given later.

The drag coefficient, based on projected frontal area, as a function of  $\beta$  is shown in Figure 2. The base flows corresponding to Regimes I and II are shown in Figure 3. In Figure 3a, for Regime I, the base flow is essentially like that of an axisymmetric body; in the mean the base flow is a closed region. In Figure 3b, for Regime II, a vortex springs from each side edge; between them there is attached longitudinal flow. In Reference 3 Carr quotes the work of Potthoff, 1969, who pointed out the existence of the side edge vortices and the fact that they can prevent the slanted base flow from separating for  $\beta$  as large as  $30^\circ$ , or even greater with suitable shaping of the body sides.

---

3. Carr, G.W., "Influence of Rear Body Shape on the Aerodynamic Characteristics of Saloon Cars", Motor Industry Research Association, Report No. 1974/2, Nuneaton, Warwickshire, February 1974.
4. Hall, M.G., "Vortex Breakdown", Annual Review of Fluid Mechanics, Vol. 4, 1972, Annual Review, Inc.
5. Leibovich, S., "The Structure of Vortex Breakdown", Annual Review of Fluid Mechanics, Vol. 10, 1978, Annual Reviews, Inc.

For Carr's model, which had a short "boat length" at the end of the slant base,  $\beta = 25^\circ$ . The surface flow pattern clearly showed the trace of the side edge vortices. A part of this pattern is sketched in Figure 4, which shows the rear view of the slanted part of the roof, i.e., slanted base. The flow along the side separates at the side edge and reattaches along the dashed line. The surface streamlines, easily visible in the oil film used for the visualization, which emanate from the dashed line, are typical of reattachment, forming what is often called a herringbone pattern close to the reattachment line. Using the reattachment line to indicate the inboard boundary of the vortex, this result shows that the vortices extend over about one-half of the width of the slant base, for this case.

There is enough evidence to conclude that side edge vortices exist for  $\beta < \beta_c$ . For smaller  $\beta$ , say  $\beta < 10^\circ$ , they probably exist but would be difficult to detect because they are weak. As pointed out by Morel <sup>1,2</sup>, the initial decrease in  $C_D$ , for  $0 < \beta < 10^\circ$ , may be a boattail type of effect, familiar in the design of projectiles, rather than a side edge vortex effect. The latter probably begins to dominate for  $\beta > 10^\circ$ . For  $\beta = \beta_c$  the discontinuity in  $C_D$  occurs and the side edge vortices disappear. This massive change in the slanted base flow field occurs suddenly, for a small change in  $\beta$ .

Before discussing the flow mechanism for this sudden change, some estimates of the side edge flow are necessary.

### III. THE SIDE EDGE FLOW

A description of the complete flow field over either of the models shown in Figure 1 by analytical methods would be very difficult. To obtain a tractable idealization the local flow at the side edge should be examined. One possibility is shown in Figure 5 where the side edge is along the x-axis and the leading edge of the slanted base, or corner, is along the y-axis. The z-axis is normal to the base and forms a right-handed, rectangular, Cartesian coordinate system. The external flow,  $U$ , is parallel to the top and side surfaces. The boundary layer would be neglected until the flow reaches the side edge and corner. This idealization, however, will not yield the simple estimates needed here.

As a further simplification, appropriate to the side edge flow away from the corner, consider an infinite, slanted, or yawed, side edge. That is, there is no corner. The side view,  $y = 0$  and the back view,  $x = \text{constant}$ , are shown in Figures 6a and 6b, respectively. The solution to this problem is independent of  $x$ . This kind of idealization is basic in the study of swept wings. As an additional approximation the incoming flow,  $U$ , is taken to be the free stream velocity over the model in Figure 1b. The thickness of the boundary layer, before it separates from the edge, is neglected. This is the same assumption made in the classical Gortler, solution for the 2-D, free, turbulent, shear layer, often called the mixing zone problem. We obtain this problem, discussed in Reference 6, if  $\beta = 90^\circ$ . This idealization of the side edge flow can be called a combination of the 2-D mixing zone solution with the sweep-back principle.

However, an additional caution must be discussed. In most applications of sweep-back theory the independence principle holds, i.e., the flow in the  $(y, z)$  plane can be computed, and then the flow in  $x$ -direction determined. For laminar flow this is always possible but, because of the Reynolds stress terms in the momentum equations, the independence principle is not strictly valid for turbulent flow. It will be assumed here that the independence principle holds; this assumption should cause a small error in the swept-back mixing zone problem.

Therefore, from Figure 6, the mixing zone flow is determined for the external velocity  $U \sin \beta$ . The velocity,  $w$ , in the  $z$ -direction, in the mixing zone is given by the well known solution<sup>6</sup>,

$$w = (1/2) U \sin \beta [1 + \operatorname{erf}(-\sigma y/z)] \quad (1)$$

where  $\sigma = 12$  is the mixing coefficient. The vorticity,  $\partial w / \partial y$ , is solely in the  $x$ -direction. The velocity parallel to the edge,  $U \cos \beta$ , is constant for all  $z$ . This is as far as the idealization can be carried. Specifically, in the absence of pressure gradients, the free shear layer cannot reattach to the wall  $z = 0$ .

On the actual model, the separated flow must reattach on the slanted base in order to form the vortex. Only empirical criteria for reattachment are available and these require knowledge of the pressure. The criterion given by Crabtree<sup>7</sup>, for leading edge bubbles on airfoils is  $S \gtrsim 0.35$  where

$$S = (C_{pr} - C_{ps}) / (1 - C_{ps}) \quad (2)$$

and  $C_{pr}$  and  $C_{ps}$  are the pressure coefficients at reattachment and separation, respectively. Using Morel's pressure data<sup>1</sup>, reattachment is indicated by Crabtree's criterion. At this stage this is only a consistency statement. It would be useful deductively if estimates of the pressure could be obtained.

The most important quantity that can be estimated from the solution to the swept-back mixing zone problem is the swirl in the side edge vortex. Assume that the flow over the actual model reattaches on the slanted base. The swirl angle is defined as

$$\phi = \tan^{-1} (v_\theta / u) \quad ,$$

---

6. White, F.M., Viscous Fluid Flow, p. 509, McGraw-Hill Book Company, New York, 1974.
7. Crabtree, L.F., "Effects of Leading-Edge Separations on Thin Wings in Two-Dimensional Incompressible Flow", I.A.S. Preprint 659, January 1957.

where  $v_\theta$  is the azimuthal velocity in the vortex and  $u$  is the velocity in the  $x$ -direction, i.e., axial velocity in the vortex.  $\phi$  varies with position in the vortex because  $v_\theta$  and  $u$  vary. The estimate for  $v_\theta$  is obtained from (1) and that for  $u$  from  $U \cos \beta$ . Thus,

$$v_\theta = 0 (U \sin \beta)$$
$$u = 0 (U \cos \beta) ,$$

so that

$$\phi = 0 (\beta) .$$

This result for  $\phi$  will be used as an approximate relation

$$\phi \approx \beta . \quad (3)$$

The velocities  $v_\theta$  and  $u$  could be measured using a laser Doppler velocimeter to obtain a check on this result.

An estimate of  $\phi$  is needed to relate breakdown of the side edge vortex to the discontinuity in  $C_D$ . The error in this estimate may be considerable; but it should decrease as  $x$  increases. Since only the ratio,  $v_\theta/u$ , is used to estimate  $\phi$  and it may have smaller error than  $v_\theta$  and  $u$ .

#### IV. THE VORTEX BREAKDOWN HYPOTHESIS

Vortex breakdown has been observed in a number of flows; e.g., flow over highly swept wings and flow in ducts. Breakdown is one of the more remarkable aspects of vortex cores. Although it has been studied vigorously, there is no completely satisfactory theory for it. The description of it given by Hall<sup>4</sup> will be quoted here; he refers to flow in a duct with swirl imparted by vanes at the duct entrance. "If we follow the fluid as it spirals along the duct we find, typically, that the structure of the vortex, as indicated for example by the velocity distribution over a cross section of the duct, varies only slowly in the axial direction and then, suddenly and, at first sight, unexpectedly, there is an abrupt change in the structure with a very pronounced retardation of the flow along the axis and a corresponding divergence of the stream surfaces near the axis." This abrupt change is called vortex breakdown. Since Hall's review many papers on the subject have appeared, too numerous to mention here. Leibovich<sup>5</sup> reviews the recent work. The important facts for present purposes are the abruptness of the change in the vortex core flow and its sensitivity to small changes in flow conditions. Vortex breakdown occurs in two forms, mainly, Reference 5. One is called the bubble type and is nearly axisymmetric, at least close to the breakdown region; the second is called the spiral type and is highly asymmetric. These are illustrated in

Figures 7a and 7b, respectively. In the duct flow a filament of dye is introduced along the axis which then gives a visual record of the breakdown.

Most of the quantitative information on vortex breakdown is obtained from duct flows because it is more difficult to run a controlled experiment in other flows. It seems that the phenomenon was first discovered in flows over highly swept wings, see Reference 4 for references and a smoke flow photograph. This photograph shows a bubble type breakdown on one side of a delta wing and a spiral type on the other. Clearly the flow over a wing, with vortices on each side of the plane of symmetry, is more representative of the slanted base flows discussed here than duct flows. For typical wings, the spanwise separation of the vortices is much greater than in slanted base flows; the interaction between the vortices is then quite different.

According to Hall<sup>4</sup> the necessary conditions for breakdown are: (1) the maximum  $\phi > 40^\circ$ ; (2) an adverse pressure gradient; (3) stream tube divergence in the vortex core. Conditions (2) and (3) are satisfied for the side edge vortices. The estimate obtained from the swept-back mixing zone problem gave  $\phi = \beta$  so that condition (1) would give  $\beta \approx 40^\circ$  for breakdown.

Condition (1) is clearly approximate. It was deduced by Hall from the limited experimental data available at the time. Since then laser-Doppler anemometry has come into wide use and is ideal for velocity measurements in vortex breakdown flow fields because no probe is introduced into the flow; a probe in the breakdown region can introduce large perturbations in the flow field. Results from many experiments on duct flows, using laser-Doppler anemometry, are presented by Leibovich<sup>5</sup>. In particular, his Table 1 summarizes data for the velocity in the approach flow, i.e., the flow to within about 1.5 vortex core diameters upstream of the breakdown point. Both bubble and spiral types of breakdown were observed and measured at three Reynolds numbers, which is based on the axial velocity far from the axis and the vortex core diameter. From that data, Table 1 was constructed.

Table 1.\*

<u>Re</u>	Type of Breakdown	$\phi_m$ (deg)	Core Expansion Ratio
1920	Spiral	31.7	1.64
	Bubble	30.4	2.54
2812	Spiral	30.6	1.78
	Bubble	30.8	1.97
3348	Spiral	33.5	2.10
	Bubble	29.9	2.76

\*Data from Reference 5.

The swirl angle,  $\phi_m$ , presented in Table is defined as

$$\phi_m \equiv \tan^{-1} (v_{\theta_{\max}} / u_{\max}) .$$

It is calculated using certain functional forms for  $v_{\theta}$  and  $u$ ; the parameters in those forms are determined from a best fit to the data. The value of  $\phi_m$  is a measure of the swirl angle for vortex breakdown; it is more reliable than the criterion given in condition (1).

In Table 1,  $\phi_m$  varies between  $29.9^\circ$  and  $33.5^\circ$ . No trend in the variation of  $\phi_m$  with Reynolds number can be detected; the average value of  $\phi_m$  is  $31.9^\circ$  for the spiral type,  $30.4^\circ$  for the bubble type, and  $31.2^\circ$  if both types are considered. For purposes of estimation,  $\phi_m = 30^\circ$  can be used. Assuming that  $\phi_m$  approximates the estimate of  $\phi$  in (3), breakdown of the side edge vortex is estimated to occur at  $\beta = 30^\circ$ .

Another feature of vortex breakdown that enters the proposed mechanism to explain the discontinuity in  $C_D$  is the increase in size of the vortex core after breakdown. Downstream of the breakdown region a new vortex is formed, in the wake region. The ratio of the wake-core radius to that in the flow upstream of breakdown is called the core expansion ratio, given in Table 1. The core radius is defined as the radial coordinate of the maximum in the azimuthal velocity. The smallest entry in the table gives a 64% increase in the size of the core.

One of the major results of the above theory is that breakdown of the side edge vortices is possible for the range of parameters covered in Morel's experiments. Assuming it does occur, its relation to the sudden change in  $C_D$  can be described as follows. Before breakdown the two vortices occupy a substantial part of the slanted base, see the discussion of Figure 4, above. The sudden billowing of these vortices, as measured by the core expansion ratio, will cause the mutual interaction between them and their interaction with the outer stream to increase. The adverse pressure gradient acting on the vortices will increase and cause the breakdown region to move further upstream, etc. Rapid movement of the breakdown region is observed in duct flow experiments. The 3-D separation pattern, or open base flow, then collapses into the quasi-axisymmetric base flow. The final stage of this collapse cannot be described by the model.

The estimates of swirl, the relationship between swirl and slant angle,  $\beta = \phi$ , and the model proposed here can now be combined. They give the critical slant angle for the discontinuity in  $C_D$ ,  $\beta_c \approx 30^\circ$ . Morel's experiments give, Figure 2,  $\beta_c = 30^\circ$ . Considering the idealizations made in arriving at the theoretical result, its agreement with the experimental value must be considered fortuitous. The proper conclusion is that the theory is consistent with the available experimental findings.

For the ogive-cylinder wind tunnel model tested by Morel<sup>2</sup>, Figure 1a, the  $C_D$  versus  $\beta$  variation was generally the same as that in Figure 2. However,

the discontinuous decrease in  $C_D$ , from 0.62 to 0.3 in this case, occurs at  $\beta_c = 43^\circ$  rather than  $\beta_c = 30^\circ$  as for the straight side-edge. Development of a flow model for the ogive-cylinder slanted base, where the edge is an ellipse, will not be attempted. Some understanding of the flow for  $\beta < \beta_c$  can be obtained by isolating three modules of the base flow field, assuming steady flow. (1) At the top of the base the flow separates. The scale of this separated region, measured by the location of reattachment line, is a small fraction of the major axis. (2) In the neighborhood of the side of the base the flow separates and side-edge vortices are formed. The flow pattern would be topologically the same as that in Figure 4. The scale of the separation region is a significant fraction of the minor axis. (3) At the bottom of the base the flow has, at most, a small scale separated region.

It appears reasonable to neglect first order interaction between these three modules; then some portion of the base surface streamlines can be sketched. For small enough  $\beta$  the side-edge vortices must depart from the base either by reaching the edge or by lifting off. It is conjectured that, for  $\beta = 30^\circ$ , either the swirl is decreased below the critical value before they depart the surface or they break down off the surface. In the former, larger  $\beta$  is required for breakdown on the surface. In the latter, their mutual interaction and that with the outer stream, which is necessary to explain the sudden change in base flow and  $C_D$ , is relatively weak. Stronger vortices, i.e., larger  $\beta$ , would be required to have breakdown on the surface and the required interaction. In either case the conclusion is consistent with the observed larger  $\beta_c$ .

## V. DISCUSSION

More refined estimates for the swirl in the side edge vortices are possible, e.g., using the configuration of Figure 5, but would require much more analysis. It would be preferable to test the central hypothesis of this theory experimentally. Introduction of a blunt body along the center of the vortex core, which is known to promote breakdown, could be useful as a diagnostic tool.

An explanation of the discontinuity in  $C_D$  at  $\beta = \beta_c$  requires a process with the abruptness (almost explosive nature) of vortex breakdown. Theories based on some other hypothesis are possible, however. One of these could be based on the inability of the free shear layer to reattach for  $\beta > \beta_c$ .

In addition to an understanding of the phenomena that lead to the discontinuity in  $C_D$ , it would be desirable to be able to predict drag, especially for  $\beta < \beta_c$ . Linearized theory might be useful for the case of small  $\beta$ . Otherwise, only numerical methods could be successful.

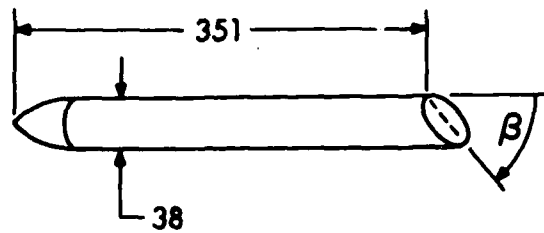
Although the discussion in this report is limited to the effect on drag of slanting the base, the phenomenon of side edge vortices and the flow model proposed for their breakdown has wider applicability. Other parts of a road vehicle have side edges and they occur in other applications. One of these is

in ballistics: the non-conical boattail proposed by Platou<sup>8</sup>. No studies of varying  $\beta$  have been made, however. A more complete understanding of the generation and breakdown of side edge vortices will be useful in many fluid dynamic problems.

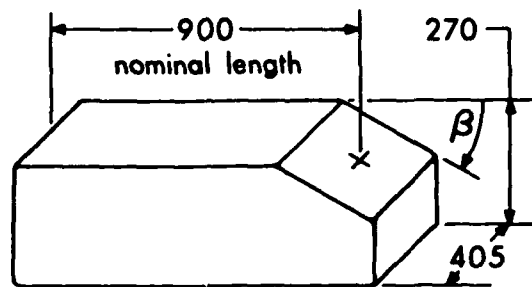
8. Platou, A.S., "An Improved Projectile Design", U.S. Army Ballistic Research Laboratory/ARRADCOM Memorandum Report No. 2395, Aberdeen Proving Ground, Maryland, July 1974. AD A785520

#### REFERENCES

1. Sovran, G., Morel, T., and Mason, W.T., Jr., Aerodynamic Drag Mechanisms of Bluff Bodies and Road Vehicles, Symposium held at the General Motors Research Laboratories, Plenum Press, New York, 1978.
2. Morel, T., "Aerodynamic Drag of Bluff Body Shapes Characteristic of Hatch-Back Cars," Research Publication GMR-2581, General Motors Research Laboratories, November 1977. See also S.A.E. Technical Paper 780267, 1978.
3. Carr, G.W., "Influence of Rear Body Shape on the Aerodynamic Characteristics of Saloon Cars," Motor Industry Research Association, Report No. 1974/2, Nuneaton, Warwickshire, February 1974.
4. Hall, M.G., "Vortex Breakdown," Annual Review of Fluid Mechanics, Vol. 4, 1972, Annual Review, Inc.
5. Leibovich, S., "The Structure of Vortex Breakdown," Annual Review of Fluid Mechanics, Vol. 10, 1978, Annual Reviews, Inc.
6. White, F.M., Viscous Fluid Flow, p. 509, McGraw-Hill Book Company, New York, 1974.
7. Crabtree, L.F., "Effects of Leading-Edge Separations on Thin Wings in Two-Dimensional Incompressible Flow," I.A.S. Preprint 659, January 1957.
8. Platou, A.S., "An Improved Projectile Design", U.S. Army Ballistic Research Laboratory/ARRADCOM Memorandum Report No. 2395, Aberdeen Proving Ground, MD, January 1974. AD A785520



(a)



(b)

Figure 1. Models Tested by Morel (2). Dimensions in mm.

- (a) Ogive-Cylinder Model
- (b) Vehicle-Like Model

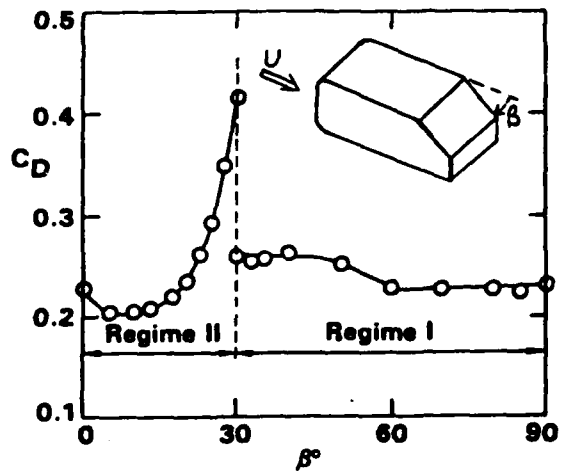
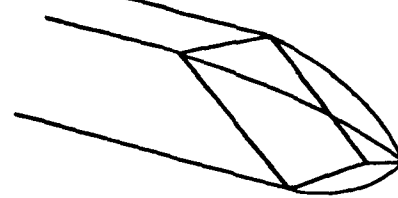


Figure 2. Drag Coefficient of the Vehicle-Like Model in the Free Stream Location, From (2)

(a) Quasi-axisymmetric Separation Pattern



(b) 3-D Separation Pattern

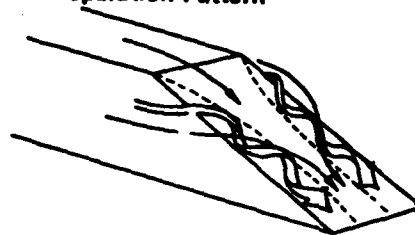


Figure 3. The Two Types of Base Flows for a Body with a Slanted Base

- (a) The Closed Type Exists in Regime I
- (b) The Open Type with Side Edge Vortices Exists in Regime II

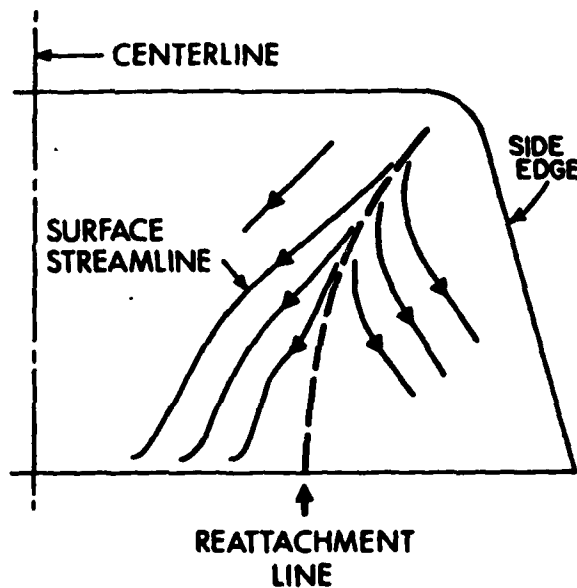


Figure 4. Rear View of a Slanted Base Showing Part of the Surface Flow Pattern. The Flow along the Side (Out of the Plane of the Paper) Separates at the Side Edge and Reattaches at the Dashed Line. Sketched from a Photograph in (3)

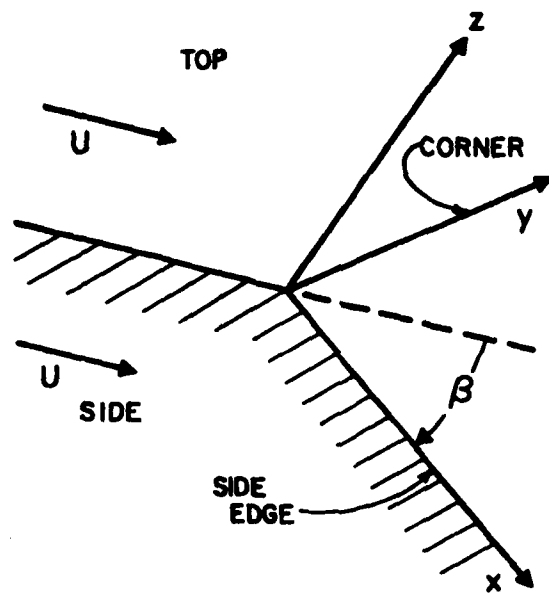


Figure 5. A Wedge, Semi-Infinite in the Y-Direction, as an Idealized Configuration for Side Edge Flow. The Free Stream Velocity,  $U$ , is Parallel to the Top and the Side. The Slanted Base is  $z = 0, x > 0, y > 0$

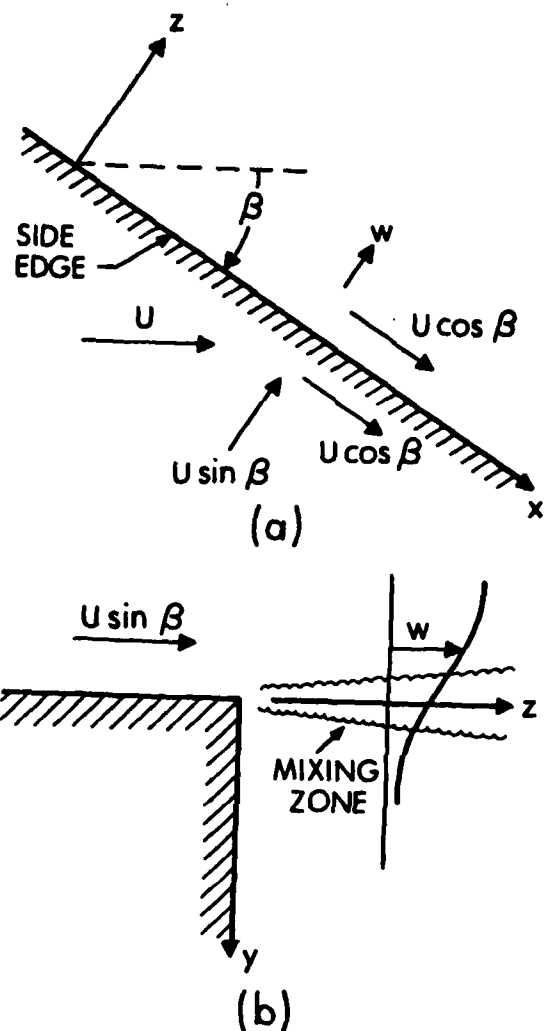


Figure 6. Flow Over an Infinite, Yawed Side Edge at  $y = 0, z = 0$

- (a) The View in the Plane  $y = 0$ .
- (b) The View in the Plane  $x = \text{constant}$ . The Flow Separates from the Side Edge, Forming a Free Shear Layer or Mixing Zone.

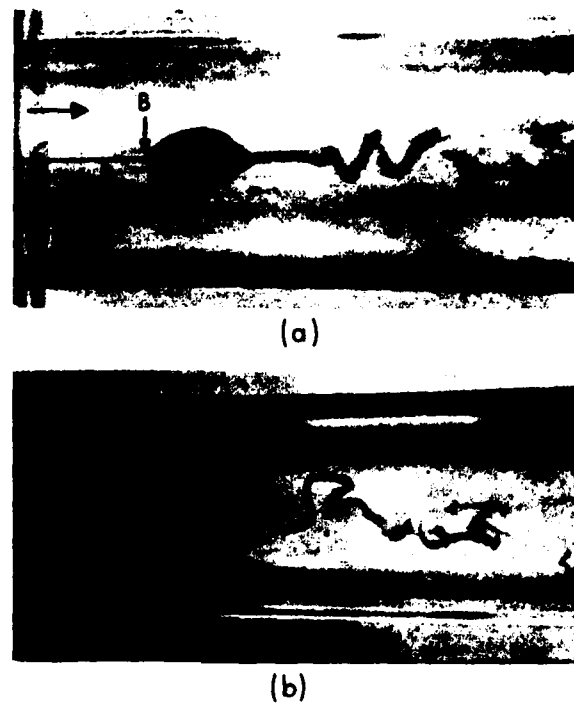


Figure 7. Vortex Breakdown in a Duct Flow, Made Visible with Dye Introduced into the Flow, From (6). B is the Breakdown Point

- (a) Bubble Type
- (b) Spiral Type

### LIST OF SYMBOLS

$C_D$	- drag coefficient based on frontal area
$C_p$	- pressure coefficient
$O$	- order of magnitude symbol
$S$	- see (2)
$u$	- axial velocity in vortex and velocity in x-direction
$U$	- free stream velocity
$v_\theta$	- azimuthal velocity in vortex
$w$	- velocity in z-direction
$x, y, z$	- Cartesian coordinates, see Figure 5
$\beta$	- angle of slanted base
$\beta_c$	- angle of slanted base dividing Regimes I and II
$\phi$	- swirl angle in vortex
$\sigma$	- mixing coefficient
<u>Subscripts</u>	
$r, s$	- reattachment and separation

DISTRIBUTION LIST

<u>No. of Copies</u>	<u>Organization</u>	<u>No. of Copies</u>	<u>Organization</u>
12	Commander Defense Technical Info Center ATTN: DDC-DDA Cameron Station Alexandria, VA 22314	1	Director US Army ARRADCOM Benet Weapons Laboratory ATTN: DRDAR-LCB-TL Watervliet, NY 12189
1	Commander US Army Engineer Waterways Experiment Station ATTN: R.H. Malter Vicksburg, MS 39180	1	Commander US Army Aviation Research and Development Command ATTN: DRDAV-E 4300 Goodfellow Blvd. St. Louis, MO 63120
1	Commander US Army Materiel Development and Readiness Command ATTN: DRCDMD-ST 5001 Eisenhower Avenue Alexandria, VA 22333	1	Director US Army Air Mobility Research and Development Laboratory ATTN: SAVDL-D, W.J. McCroskey Ames Research Center Moffett Field, CA 94035
3	Commander US Army Armament Research and Development Command ATTN: DRDAR-TSS (2 cys) DRDAR-LC, Dr. J. Frasier Dover, NJ 07801	1	Commander US Army Communications Rsch and Development Command ATTN: DRDCO-PPA-SA Fort Monmouth, NJ 07703
6	Commander US Army Armament Research and Development Command ATTN: DRDAR-LCA-F Mr. D. Mertz Mr. E. Falkowski Mr. A. Loeb Mr. R. Kline Mr. S. Kahn Mr. S. Wasserman Dover, NJ 07801	1	Commander US Army Electronics Research and Development Command Technical Support Activity ATTN: DELSD-L Fort Monmouth, NJ 07703
1	Commander US Army Armament Materiel Readiness Command ATTN: DRSAR-LEP-L, Tech Lib Rock Island, IL 61299	3	Commander US Army Missile Command ATTN: DRSMI-R DRSMI-YDL DRSMI-RDK Mr. R. Deep Redstone Arsenal, AL 35809
		1	Commander US Army Tank Automotive Research & Development Cmd ATTN: DRDTA-UL Warren, MI 48090

DISTRIBUTION LIST

<u>No. of Copies</u>	<u>Organization</u>	<u>No. of Copies</u>	<u>Organization</u>
1	Commander US Army Jefferson Proving Ground ATTN: STEJP-TD-D Madison, IN 47250	1	Commander Naval Surface Weapons Center ATTN: DX-21, Lib Br Dahlgren, VA 22448
1	Commander US Army Research Office ATTN: Dr. R.E. Singleton P.O. Box 12211 Research Triangle Park, NC 27709	5	Commander Naval Surface Weapons Center Applied Aerodynamics Division ATTN: K.R. Enkenhus M. Ciment S.M. Hastings A.E. Winklemann W.C. Ragsdale Silver Spring, MD 20910
1	AGARD-NATO ATTN: R.H. Korkegi APO New York 09777	1	AFATL (DLDL, Dr. D.C. Daniel) Elgin AFB, FL 32542
1	Director US Army TRADOC Systems Analysis Activity ATTN: ATAA-SL, Tech Lib White Sands Missile Range, NM 88002	2	AFFDL (W.L. Hankey; J.S. Shang) Wright-Patterson AFB, OH 45433
3	Commander Naval Air Systems Command ATTN: AIR-604 Washington, DC 20360	4	Director National Aeronautics and Space Administration ATTN: D.R. Chapman J. Rakich W.C. Rose B. Wick Ames Research Center Moffett Field, CA 94035
3	Commander Naval Ordnance Systems Command ATTN: ORD-0632 ORD-035 ORD-5524 Washington, DC 20360	4	Director National Aeronautics and Space Administration ATTN: E. Price J. South J.R. Sterrett Tech Library Langley Research Center Langley Station Hampton, VA 23365
2	Commander David W. Taylor Naval Ship Research & Development Cmd ATTN: H.J. Lugt, Code 1802 S. de los Santos Head, High Speed Aero Division Bethesda, MD 20084	1	Director National Aeronautics and Space Administration Lewis Research Center ATTN: MS 60-3, Tech Lib 21000 Brookpark Road Cleveland, OH 44135

### DISTRIBUTION LIST

<u>No. of Copies</u>	<u>Organization</u>	<u>No. of Copies</u>	<u>Organization</u>
2	Director National Aeronautics and Space Administration Marshall Space Flight Center ATTN: A.R. Felix, Chief S&E-AERO-AE Dr. W.W. Fowlis Huntsville, AL 35812	1	Center for Interdisciplinary Programs ATTN: Victor Zakkay W. 177th Street & Harlem River Bronx, NY 10453
2	Director Jet Propulsion Laboratory ATTN: L.M. Mach Tech Library 4800 Oak Grove Drive Pasadena, CA 91103	1	General Dynamics ATTN: Research Lib 2246 P.O. Box 748 Fort Worth, TX 76101
3	Arnold Research Org., Inc. ATTN: J.D. Whitfield R.K. Matthews J.C. Adams Arnold AFB, TN 37389	1	General Electric Company, RESD ATTN: R.A. Larmour 3198 Chestnut Street Philadelphia, PA 19101
3	Aerospace Corporation ATTN: T.D. Taylor H. Mirels R.L. Varwig Aerophysics Lab. P.O. Box 92957 Los Angeles, CA 90009	2	Grumman Aerospace Corporation ATTN: R.E. Melnik L.G. Kaufman Bethpage, NY 11714
1	AVCO Systems Division ATTN: B. Reeves 201 Lowell Street Wilmington, MA 01887	2	Lockheed-Georgia Company ATTN: B.H. Little, Jr. G.A. Pounds Dept 72074, Zone 403 86 South Cobb Drive Marietta, GA 30062
3	Boeing Commerical Airplane Company ATTN: G.M. Bowes M.S. 1W-82, Org 6-8340 P.E. Rubbert, MS 3N-29 J.D. McLean, MS 3N-19 Seattle, WA 98124	1	Lockheed Missiles and Space Company ATTN: Tech Info Center 3251 Hanover Street Palo Alto, CA 94304
3	Calspan Corporation ATTN: A. Ritter G. Homicz W. Rae P.O. Box 400 Buffalo, NY 14221	3	Martin-Marietta Laboratories ATTN: S.H. Maslen S.C. Traugott H. Obremski 1450 S. Rolling Road Baltimore, MD 21227
		2	McDonnell Douglas Astronautics Corporation ATTN: J. Xerikos H. Tang 5301 Bolsa Avenue Huntington Beach, CA 92647

DISTRIBUTION LIST

<u>No. of Copies</u>	<u>Organization</u>	<u>No. of Copies</u>	<u>Organization</u>
2	McDonnell-Douglas Corporation Douglas Aircraft Company ATTN: T. Cebeci K. Stewartson 3855 Lakewood Boulevard Long Beach, CA 90801	2	Illinois Institute of Tech ATTN: M.V. Morkovin H.M. Nagib 3300 South Federal Chicago, IL 60616
2	Sandia Laboratories ATTN: F.G. Blottner Tech Lib Albuquerque, NM 87115	1	The Johns Hopkins University Department of Mechanics and Materials Science ATTN: S. Corrsin Baltimore, MD 21218
2	United Aircraft Corporation Research Laboratories ATTN: M.J. Werle Library East Hartford, CT 06108	1	The Johns Hopkins University Applied Physics Laboratory ATTN: R.D. Whiting Johns Hopkins Road Laurel, MD 20810
1	Vought Systems Division LTV Aerospace Corporation ATTN: J.M. Cooksey Chief, Gas Dynamics Lab, 2-53700 P.O. Box 5907 Dallas, TX 75222	1	Louisiana State University Department of Physics ATTN: R.G. Hussey Baton Rouge, LA 70803
1	Arizona State University Department of Mechanical and Energy Systems Engineering ATTN: G.P., Neitzel Tempe, AZ 85281	3	Massachusetts Institute of Technology ATTN: E. Covert H. Greenspan Tech Lib 77 Massachusetts Avenue Cambridge, MA 02139
3	California Institute of Technology ATTN: Tech Library H.B. Keller, Mathematics Dept. D. Coles, Aeronautics Dept. Pasadena, CA 91109	2	North Carolina State Univ Mechanical and Aerospace Engineering Department ATTN: F.F. DeJarnette J.C. Williams Raleigh, NC 27607
1	Cornell University Graduate School of Aero Engr ATTN: Library Ithaca, NY 14850	1	Notre Dame University Department of Aero Engr ATTN: T.J. Mueller South Bend, IN 46556

DISTRIBUTION LIST

<u>No. of Copies</u>	<u>Organization</u>	<u>No. of Copies</u>	<u>Organization</u>
2	Ohio State University Dept of Aeronautical and Astronautical Engineering ATTN: S.L. Petrie O.R. Burggraf Columbus, OH 43210	1	Southern Methodist University Department of Civil and Mechanical Engineering ATTN: R.L. Simpson Dallas, TX 75275
2	Polytechnic Institute of New York ATTN: G. Moretti S.G. Rubin Route 110 Farmingdale, NY 11735	1	Southwest Research Institute Applied Mechanics Reviews 8500 Culebra Road San Antonio, TX 78228
3	Princeton University James Forrestal Research Ctr Gas Dynamics Laboratory ATTN: S.M. Bogdonoff S.I. Cheng Tech Library Princeton, NJ 08540	1	University of California- Berkeley Department of Aerospace Engineering ATTN: M. Holt Berkeley, CA 94720
1	Purdue University Thermal Science & Prop Center ATTN: Tech Library W. Lafayette, IN 47907	1	University of California- Davis ATTN: H.A. Dwyer Davis, CA 95616
1	Rensselaer Polytechnic Institute Department of Math. Sciences ATTN: R.C. DiPrima Troy, NY 12181	2	University of California- San Diego Department of Aerospace Engineering and Mechanical Engineering Sciences ATTN: P. Libby Tech Library La Jolla, CA 92037
1	Rutgers University Department of Mechanical, Industrial and Aerospace Engineering ATTN: R.H. Page New Brunswick, NJ 08903	1	University of Cincinnati Department of Aerospace Engineering ATTN: R.T. Davis Cincinnati, OH 45221
1	San Diego State University Department of Aerospace Engr and Engr Mechanics College of Engineering ATTN: K.C. Wang San Diego, CA 92182	1	University of Colorado Department of Astro-Geophysics ATTN: E.R. Benton Boulder, CO 80302
		1	University of Hawaii Dept of Ocean Engineering ATTN: G. Venezian Honolulu, HI 96822

DISTRIBUTION LIST

<u>No. of Copies</u>	<u>Organization</u>	<u>No. of Copies</u>	<u>Organization</u>
2	University of Maryland ATTN: W. Melnik J.D. Anderson College Park, MD 20740	1	University of Wyoming ATTN: D.L. Boyer University Station Laramie, WY 82071
2	University of Michigan Department of Aeronautical Engineering ATTN: W.W. Wilmarth Tech Library East Engineering Building Ann Arbor, MI 48104	1	Virginia Polytechnic Institute and State University Department of Aerospace Engineering ATTN: Tech Library Blacksburg, VA 24061
1	University of Santa Clara Department of Physics ATTN: R. Greeley Santa Clara, CA 95053	1	Woods Hole Oceanographic Institute ATTN: J.A. Whitehead Wolds Hole, MA 02543
3	University of Southern California Department of Aerospace Engineering ATTN: T. Maxworthy P. Weidman L.G. Redekopp Los Angeles, CA 90007	<u>Aberdeen Proving Ground</u>	
1	University of Texas Department of Aerospace Engineering ATTN: J.C. Westkaemper Austin, TX 78712	Dir, USAMSA	ATTN: DRXSY-D DRXSY-MP, H. Cohen
1	University of Virginia Department of Aerospace Engineering & Engineering Physics ATTN: I.D. Jacobson Charlottesville, VA 22904	Cdr, USATECOM	ATTN: DRSTE-TO-F
1	University of Washington Department of Mechanical Engineering ATTN: Tech Library Seattle, WA 98195	Cdr/Dir, USA CSL	ATTN: Munitions Div, Bldg. E3330 E.A. Jeffers W.C. Dee W.J. Pribyl
		Dir, USACSL	ATTN: DRDAR-CLB-PA M. Miller

### USER EVALUATION OF REPORT

Please take a few minutes to answer the questions below; tear out this sheet, fold as indicated, staple or tape closed, and place in the mail. Your comments will provide us with information for improving future reports.

1. BRL Report Number \_\_\_\_\_

2. Does this report satisfy a need? (Comment on purpose, related project, or other area of interest for which report will be used.)  
\_\_\_\_\_  
\_\_\_\_\_  
\_\_\_\_\_

3. How, specifically, is the report being used? (Information source, design data or procedure, management procedure, source of ideas, etc.)  
\_\_\_\_\_  
\_\_\_\_\_  
\_\_\_\_\_

4. Has the information in this report led to any quantitative savings as far as man-hours/contract dollars saved, operating costs avoided, efficiencies achieved, etc.? If so, please elaborate.  
\_\_\_\_\_  
\_\_\_\_\_  
\_\_\_\_\_

5. General Comments (Indicate what you think should be changed to make this report and future reports of this type more responsive to your needs, more usable, improve readability, etc.)  
\_\_\_\_\_  
\_\_\_\_\_  
\_\_\_\_\_

6. If you would like to be contacted by the personnel who prepared this report to raise specific questions or discuss the topic, please fill in the following information.

Name: \_\_\_\_\_

Telephone Number: \_\_\_\_\_

Organization Address: \_\_\_\_\_  
\_\_\_\_\_  
\_\_\_\_\_

DAI  
FILM